

NPS-51Es74011A

# NAVAL POSTGRADUATE SCHOOL

## Monterey, California



A QUASI-EMPIRICAL MODEL  
OF THE  
HURRICANE BOUNDARY LAYER

Russell L. Elsberry  
Nils A. S. Pearson  
Leino B. Corgnati, Jr.

Approved for public release, distribution unlimited

31 January 1974



NAVAL POSTGRADUATE SCHOOL  
Monterey, California


Rear Admiral M. B. Freeman  
Superintendent

J. R. Borsting  
Academic Dean

ABSTRACT

A numerical model of the hurricane boundary layer is described and evaluated. It is proposed that the model be coupled with an ocean model to study hurricane-ocean interaction.

This task was supported by:      Environmental Prediction Research Facility  
   Monterey, California  
   and  
   Office of Naval Research





## ABSTRACT

Solutions have been obtained for the temperature and moisture distributions within the atmospheric boundary layer of an axisymmetric hurricane model. The intensity of the hurricane is related to the equivalent potential temperature gradient produced by a balance of heat sources and advection within the boundary layer. Solutions are obtained using the bulk aerodynamic transport equations or applying a two-layer, baroclinic boundary layer model by Cardone (1969). Equilibrium maximum wind speeds vary from minimal hurricane force to about 80 m/sec for fixed ocean temperatures between 27C and 31C. Observations of the oceanic heat loss in actual storms are necessary to establish the ratio of heat flux to momentum transfer in the high wind speeds treated by the model. Various applications of the model are proposed, with an ultimate goal of a time-dependent simulation of hurricane-ocean coupling.

## INTRODUCTION

A number of axisymmetric vortex models (e.g., Yamasaki, 1968a and 1968b; Ooyama, 1969; Rosenthal, 1971) have been developed to describe the evolution of the intense wind region characteristic of hurricanes. The specified initial conditions are mainly designed to insure low-level inflow, so that the vortex will eventually become unstable, and are not related to observations. As a result, a comparatively long "organizational period" is required before deepening of the vortex ensues. A primary result of these models is the very realistic simulation of the wind structure near the center of the hurricane. Because the initial conditions are arbitrarily specified, rather than from real data, the intermediate stages of the vortex simulation may not be realistic. These models do not allow forcing by external circulations.

Instead, the philosophy is to displace the exterior boundaries of the model as far as necessary to assure that the boundary conditions will not affect the solution near the center. A complete assessment of external circulations, and other asymmetric effects, on hurricane simulation must await further development (see Anthes et al, 1971) of three-dimensional models started with real initial data.

The objective of this paper is to describe a simplified model of the properties within the hurricane boundary layer. Although the ultimate purpose is to simulate the time variation of these properties due to changes in sea-surface temperatures, in the present paper the emphasis will be on the adjustment to different fixed sea-surface temperatures. It is well known that tropical storms develop into hurricanes only over warm tropical oceans. Indeed the oceanic surface layers must provide the heat necessary to produce the unique warm core of the mature hurricane. The preferential release of the heat in deep convective towers near the hurricane eye results in central temperatures much higher than the environment. To a first approximation, the heat gain within the boundary layer may be linearly related to the tangential wind speed at the top of the layer ( $v_\theta$ ), but the frictional loss of momentum to the ocean increases as  $v_\theta^2$ . Thus a given radial profile of wind speed essentially specifies the heat gain which sustains the hurricane, as well as the frictional loss which tends to offset further increases in wind speed. On this basis, Riehl (1963) developed relations for the unique wind profile (and associated thermal structure) for which these offsetting tendencies are in balance; that is, for the conditions in which a steady state hurricane should result. However, an actual storm may not reach its full potential, or may be in steady state for only a short time, because the characteristics of the ocean and surrounding environment vary in space and time. A prime motivation of this study was to develop a model capable of simulating the symmetric component of actual storms.

## DESCRIPTION OF THE MODEL

The empiricism of the model is based on three assumptions. First, the wind profile at the top of the boundary layer is specified by the relation

$$v_{\theta} r^{1/2} = \text{constant} , \quad (1)$$

outside the radius of maximum wind speed ( $r_i$ ). Between the vortex center and  $r_i$  the winds are assumed to obey  $v_{\theta} r^{-1} = \text{constant}$ , which represents solid-body rotation. Justification of (1) was given by Gray and Shea (1973) who found an exponent of  $0.47 \pm 0.30$  in  $v_{\theta}$  profiles from hurricanes in various stages of development. Rather than using individual  $v_{\theta}$  profiles, Riehl (1963) averaged profiles around the storm and found the exponent (1/2) applied in many cases, particularly in quasi-steady state hurricanes. Some of the additional variation which Gray and Shea found must be due to transient features in the wind field as the storm adjusts to varying internal or external conditions. In simulating the free-atmosphere as a series of "equilibrium states" represented by (1), these transient features are assumed to be of less importance than the symmetrical circulation. It should be emphasized that the coefficient in (1) was determined from aircraft data only within about 150 km of the center. This is the region in which the symmetry assumption is most justifiable, and, fortunately, is the primary region of interest in evaluating the effects of the hurricane. Lack of systematic observations at larger radii prevent an accurate description of the outer region in which the external effects are likely to be manifested in actual hurricanes. Therefore, beyond  $r_o$  [defined in (5)] the exponent in (1) was adjusted to always reduce the wind speed at  $2r_o$  to  $5 \text{ m sec}^{-1}$ . Specifying a different exponent in the outer region had an insignificant effect on the properties near the center compared to experiments in which (1) was applied throughout the region.



The second empirical formula relates the maximum wind speed to the increase in the equivalent potential temperature of the boundary layer ( $\delta\theta_e$ ) due to the oceanic heat source. Such a relation was proposed by Riehl (1963), through the use of the cyclostrophic assumption and observations relating the surface pressure at the radius of maximum wind to  $\delta\theta_e$ ,

$$\delta p = - 2.5 \delta\theta_e, \quad (2)$$

where the  $\delta$  symbols indicate deviations from  $p = 1005$  and  $\theta_e = 350K$ . In the present model, a gradient wind expression

$$\frac{1}{\rho} \frac{\partial p}{\partial r} = v_\theta \left( f + \frac{v_\theta}{r} \right) \quad (3)$$

was used instead of the cyclostrophic assumption. Although Ooyama (1969) showed that the inertial term is important near the surface, this term may be dropped if (3) is averaged over the depth of the boundary. Upon integration of (3) between the radii over which (2) applies, the tangential component ( $v_{\theta_i}$ ) at the radius of maximum wind ( $r_i$ ) is

$$v_{\theta_i} = \frac{0.5 r_o}{r_o - r_i} \left[ -2f(\sqrt{r_i r_o} - r_i) + \sqrt{4f^2(\sqrt{r_i r_o} - r_i)^2 + 10^6 \frac{r_o - r_i}{\rho r_o} (\theta_{e_i} - \theta_{e_o})} \right] \quad (4)$$

The dominant term in this expression is that involving the difference in  $\theta_e$  at  $r_i$  and at some radius  $r_o$  where  $p = 1005$  and  $\theta_e = 350K$ , which follows from (2). Bell and Tsui (1973) found a similar relation between pressure and  $\theta_e$  changes for tropical cyclones near the Asian coast, but with a coefficient of 2.25. Because of the difficulty in establishing the desired surface pressure at  $r_i$ , and only a 10% percent difference, the coefficient in (2) was adopted. It is clear from (4) that the radius of maximum wind ( $r_i$ ) should coincide with the maximum  $\theta_e$  within the boundary layer. In the



present model,  $r_i$  was chosen as the radius at which  $\theta_e$ , averaged over five grid increments ( $\Delta r = 3\text{km}$ ), was a maximum. This assumption makes  $r_i$  coincident with the eyewall clouds, because the boundary layer air parcels with the largest heat and moisture content would be expected to be most favorable for deep convection. Shea and Gray (1973) show that  $r_i$  tends to be coincident with the eyewall in the most intense hurricanes, but  $r_i$  is larger than the eyewall radius in weaker storms. The radius ( $r_o$ ) at which  $p = 1005$  and  $\theta_e = 350\text{K}$  may be taken to represent an external influence, and must be defined in terms of other parameters. As the  $p$  and  $\theta_e$  gradients are small outside the central region, the inaccuracy in specifying  $r_o$  is a second-order effect compared with  $r_i$ . For convenience we choose

$$r_o = \left( \frac{2}{f} v_{\theta_i} r_i \right)^{1/2} \quad (5)$$

which is approximately the radius at which  $v_{\theta}$  tends to zero in the outflow layer of the storm, if the air originating in the maximum wind region conserves absolute angular momentum. Since  $r_o$  is about  $200\text{km}$  for  $f \sim 5(10^{-5})\text{sec}^{-1}$  and typical values of  $v_{\theta_i}$  and  $r_i$ , this again represents the region of application of the model. A schematic representation of the wind structure in the atmospheric vortex is given in Figure 1.

The above relations represent an empirical model of the wind speeds in hurricanes as a function of the  $\theta_e$  distribution within the boundary layer. Rather than determine the maximum  $\theta_e$  from observations as proposed by Riehl (1963), the  $\theta_e$  fields will be calculated from time-dependent equations for the potential temperature ( $\theta$ ) and specific humidity ( $q$ ),

$$\theta_e = \theta \exp \left( \frac{Lq}{C_p T} \right)$$

$$\frac{\partial \theta}{\partial t} = - \frac{\partial (r v_r \theta)}{r \partial r} - \frac{\partial (\omega \theta)}{\partial p} + \frac{g Q_s}{C_p \Delta p}, \text{ and} \quad (6)$$

$$\frac{\partial q}{\partial t} = - \frac{\partial (rv_r q)}{r \partial r} - \frac{\partial (\omega q)}{\partial p} + \frac{g Q_e}{L \Delta p} . \quad (7)$$

In these equations  $C_p$  and  $L$  are the specific heat and latent heat of vaporization. Only the symmetrical circulation is considered, so that the radial ( $v_r$ ) and vertical ( $\omega$ ) components of motion are related by

$$\frac{\partial \omega}{\partial p} = - \frac{\partial rv_r}{r \partial r} , \quad (8)$$

with the further approximation that  $\omega = 0$  at the surface. Radiative exchanges are assumed to be negligible and the sensible ( $Q_s$ ) and latent ( $Q_e$ ) heat fluxes are assumed to decrease to zero within  $\Delta p = 100$  mb of the surface. The actual vertical heat fluxes through the top of the boundary layer are determined by the mean flow represented by  $\omega$  and convective towers. Normally the convective heat flux is parameterized in terms of the mean flow; however, this resulted in supersaturation in the present model, as was the experience of Rosenthal (1971). The third important empirical aspect of the model was the formulation of a critical relative humidity profile, such that the moisture in excess of the critical value was arbitrarily removed from the boundary layer. The convective heat flux  $\omega \theta$  was neglected.

Because the radial gradient of  $\theta_e$  is essentially determined by the moisture gradient, the specification of the critical relative humidity profile was a primary factor in determining the intensity of the model hurricane. As a first attempt, the critical relative humidity for the air in the exterior region was specified as the value which would produce a lifting condensation level (LCL) of 60 mb above the surface. A decrease in the typical cloud base height toward the center is commonly observed in hurricanes, although the magnitude of the decrease has not been documented as a function of maximum wind speed. In this case, a linear decrease to a LCL of 30 mb at the eyewall

was assumed. Profiles other than a linear decrease were also used, but these did not change the results. These LCL values corresponded to external and internal critical relative humidity values of about 77 and 88%, respectively, for the range of sea surface temperatures used here. These values seem realistic as one might expect the external air to be somewhat drier because of subsidence, and the interior air to be more moist than normal (about 80% in the subcloud layer). In the second approach, the critical relative humidity values were arbitrarily specified as a linear profile between 95% inside  $r_i$  and 75% outside  $r_o$ . These values might be taken as representative of the maximum conditions one might expect, and the results for this specification will be referred to as the maximum hurricane. A 95% value implies a cloud base of about 150 m near the center.

#### BOUNDARY LAYER MODELS

The surface fluxes  $Q_s$ ,  $Q_e$  and  $\tau_{\theta s}$  required to close the solutions are determined by the boundary layer model. For fixed oceanic conditions, the model will tend to steady state as the radial and vertical advection of heat and moisture within the boundary layer balance the oceanic sources  $Q_s$  and  $Q_e$ , respectively. In this formulation the air-sea temperature and humidity differences will vary with radius as determined from (6) and (7). The first approach to the boundary layer was to assume the bulk aerodynamic equations for momentum, heat and moisture fluxes:

$$\tau_{\theta s} = \rho C_D V_s v_{\theta s} \quad (9)$$

$$Q_s = C_p \rho C_H V_s (T_w - T) \quad (10)$$

$$Q_e = L \rho C_H V_s (q_w - q) \quad (11)$$

$$C_D = \frac{3}{2} C_H = 1.1 \times 10^{-3} + 4 \times 10^{-5} |V_s|$$

where  $C_H$  is the heat/moisture exchange coefficient,  $\tau_{\theta s}$  is the surface shearing stress,  $q_w$  is the specific humidity corresponding to the saturation vapor pressure at the sea surface temperature  $T_w$ , and the total wind speed ( $V_s$ ) is 0.7 times the wind speed at the top of the boundary layer. If the shearing stress vanishes at the top of the boundary layer, the steady-state, tangential equation of motion may be used to determine the mean radial flow within the layer,

$$v_r = \frac{\tau_{\theta s} / \Delta p}{\left(f + \frac{\partial v_\theta}{\partial r} + \frac{v_\theta}{r}\right)} \quad (12)$$

The set (1) - (12) is thus closed for a given sea surface temperature, and may be solved as an initial value problem.

As an alternative to the bulk aerodynamic equation approach, a two-layer, baroclinic model developed by Cardone (1969) was adopted. The Cardone model of the marine boundary layer, hereafter referred to as CBL, was an extension of the neutral, fixed-terrain model described by Blackadar (1965). The two-layer CBL model is schematically illustrated in Figure 2. In the surface layer the eddy viscosity ( $K_M$ ) is a function of height and atmospheric stability, according to the Monin-Obukhov similarity theory. Specifying a constant  $K_M$ , equal to its value at the top of the surface layer, and replacing  $f$  by  $(f + v_\theta/r)$ , results in a modified Ekman spiral in the upper layer. Following Cardone (1969), the surface roughness ( $Z_o$ ) in meters is internally determined as a function of the friction velocity ( $u_*$ ),

$$Z_o = \frac{6.84(10^{-5})}{u_*} + 4.28(10^{-3})u_*^2 - 4.43(10^{-4}) \quad (13)$$

The desired boundary layer wind profiles and associated heat flux can be determined from the solution of the following set of simultaneous

equations,

$$C_D = \sqrt{2} k \sin \left( \frac{\pi}{4} - \alpha_o \right) / [\ln B_o R_o - \psi(L_*)] \quad (14)$$

$$C_D^3 = 2 k B_o \sin^2 \alpha_o / \phi(L_*) \quad (15)$$

where

$C_D = u_*/V_g$ , the geostrophic drag coefficient,

$k = 0.4$ , von Karman's constant,

$\alpha_o$  = surface cross-isobaric angle,

$R_o = V_g/fZ_o$ , surface Rossby number,

$\phi(L_*)$  = non-dimensional wind shear function,

$\psi(L_*)$  = wind profile function,

$L_* = h/L'$ , stability index,

$h = B_o V_g / [f + v_\theta/r]$ , height of constant flux layer,

$B_o = 3 \times 10^{-4}$ , dimensionless constant,

$L' = a_h^{-1} u_*^2 \bar{\theta} [\ln(10/Z_o) - \psi(10/L')] / [gk^2(T_{va} - T_{vs})]$ , the

gradient form of the Monin-Obukhov length applied at 10 m,

$a_h = K_H/K_M$  ratio of the heat transfer coefficient to the eddy viscosity,

$\bar{\theta}$  = mean potential temperature in the boundary layer, and

$T_{va} - T_{vs}$  = virtual temperature difference between 10 m and the sea surface.

Expressions for  $\phi(L_*)$  and  $\psi(L_*)$  and the iterative method for solving the highly implicit set (13) - (15) are given by Cardone (1969). Solutions for  $u_*$ ,  $\alpha_o$  and  $L'$  specify the desired wind profiles and implied heat flux in the constant flux layer. It should be noted that the virtual temperature difference  $(T_{va} - T_{vs})$  is used to represent both sensible ( $Q_s$ ) and latent ( $Q_e$ ) fluxes from



$$H = Q_s + Q_e = [-u_*^3 C_p \rho a_h \bar{\theta}] / [\text{kg L}'] \quad (16)$$

Individual  $Q_s$  and  $Q_e$  fluxes are specified according to the ratio  $(T_w - T) / (q_w - q)$ . The radial wind component was determined by integrating the wind profile given by the similarity theory at four points within the constant flux layer and by the modified Ekman spiral above.

Use of the CBL in the atmospheric vortex assumes applicability of the similarity theory in wind regimes for which observations are lacking. Thus the model results must be critically examined; hopefully, the results will stimulate interest in devising and obtaining the measurements necessary to improve the boundary layer representation under hurricane conditions.

Computational aspects. The combined vortex-boundary layer model was solved as an initial value problem with centered space and time-differences after an initial forward step. Forward time steps were also used periodically to reduce the time separation of the solutions. Ocean temperature values were constant in space and time. Because the model is to be started from non-zero initial wind speeds, temperature and moisture fields that are consistent with the vortex intensity must be specified. Although an estimate of  $\theta_e$  along the radius may be obtained from (2) - (4) using the  $v_\theta$  profile, the values of  $\theta$  (or  $T$ ) and  $q$  must also be consistent with the heat/moisture source and the advection. As sufficient data were not available to specify all of these variables, two techniques were used to specify initial values. In the first experiments the relative humidity was specified and the Clausius-Clapeyron equation and the  $\theta_e$  definition were solved iteratively for the temperature. An alternative approach was to relate the atmospheric temperature to the oceanic temperature, and to determine the specific humidity from the  $\theta_e$  value calculated from (2) - (4). Thus in regions where the initial air temperature was too high, the initial  $q$  field was too low. If

the ocean temperature were fixed, the radial temperature and humidity profiles approached the same values within a few hours with both initialization techniques. Consequently, the second alternative was adopted by specifying an air temperature 1C less than the ocean temperature.

## RESULTS

### Effect of Ocean Temperature

A comparison of the maximum tangential wind speed for the two critical relative humidity specifications is shown in Table 1 for the two boundary layer versions. In both cases there is a systematic increase in maximum  $v_\theta$  as the sea surface temperature is increased. Ooyama (1969) also found a change of about  $20 \text{ m sec}^{-1}$  for a 2C change in sea temperature. When the moisture specification dependent on the cloud base is used, minimal hurricane-force winds are obtained for an ocean temperature of 28C. With the maximum relative humidity specified as 95%, hurricane-force winds are obtained with a sea temperature of 27C. Similar differences in maximum wind speed are obtained at the same ocean temperature for the two moisture specifications, irrespective of the boundary layer model. The differences caused by the moisture specification decrease slowly with increasing sea surface temperature.

Riehl (1963) noted the threshold  $\theta_e$  value for producing surface pressures capable of sustaining tropical storms and hurricanes was 350K. Parcels with surface properties corresponding to  $\theta_e > 350\text{K}$  are required for deep convection and warming of the tropospheric column. For higher oceanic temperature, the air temperatures and specific humidities throughout the boundary layer are increased. Thus the environmental  $\theta_e$  values (at  $r_o$ ) tended to increase along with the values near the eyewall. An increase in  $\theta_e$  at  $r_i$  relative to  $\theta_e$  at  $r_o$  is associated with a pressure decrease as specified in (2), and also with the maximum wind through (4). However, the  $\theta_e$  of the environmental



air exceeds 350K for the experiments with high ocean temperatures. If only the increase in  $\theta_e$  over the value at  $r_j$  is assumed to contribute to the surface pressure drop, the maximum wind speeds shown in parentheses in Table 1 result. Only a small increase in wind speed is predicted for water temperatures above 30C. Within the framework of three basic assumptions of the model, such an interpretation would suggest a plateau of maximum intensity of storms regardless of water temperature in excess of a certain value. For a 95% specification of the critical relative humidity at the eyewall, the  $\delta\theta_e$  values are about 13-15K over the entire range of ocean temperatures in Table 1. Wind speeds exceeding the plateau value could only be expected if anomalously cool and dry conditions existed around a tropical storm over a warm ocean. Such conditions might be expected as the storm nears a coastal region, if the inflowing boundary layer air originating over land has a sufficiently long trajectory over water before entering the central regions of the storm. One can speculate that the combination of a favorable environment and the warm coastal waters could lead to intensification near the coast, prior to the filling phase after the storm center crosses the coast.

It is somewhat satisfying that the crude representation in terms of the bulk aerodynamic transport equations produces maximum intensities which are quite similar to those obtained from the more sophisticated CBL. The CBL, incorporating the empirical constants as specified by Cardone (1969), does appear to be slightly more sensitive to the sea surface temperature variations. The similarity of the results is closely related to the critical relative humidity specification, since both boundary layer versions have large evaporation rates which necessitate the parameterization of convective clouds. In this sense the external parameters are dominant and

other measures must be used to compare the internal parameters of the two models.

#### Model Parameter Distributions

One of the objectives of the model formulation was to determine equilibrium atmospheric conditions for given ocean temperatures, rather than simply specifying fixed air-sea temperature and moisture differences. Values of sea-air temperature differences are shown in Figure 3, for the CBL with a maximum relative humidity of 95%. Over most of the region the surface air temperature remains essentially constant. A somewhat larger sea-air temperature difference is predicted in more intense storms that occur with higher ocean temperatures. Near the central region, the air temperature decreases rapidly. In the minimum hurricane (27C) the temperature decrease is to a value 1C below the water temperature, but for the most intense (31C) storm the decrease is more than 4C. Riehl (1963) used a constant difference of 2.5C for the region with wind speeds exceeding  $25 \text{ m sec}^{-1}$ . Bell and Tsui (1973) found the mean air temperature for 60 ship observations within 100 n mi of the center was 1.2C less than the ocean temperature. A 5C difference was observed as the center of hurricane Hilda passed with 40 n mi of the NOMAD buoy (see Marcus and Smith, 1966). Thus, one might conclude that the air-sea temperature differences from the model are not inconsistent with the variation determined from the few available observations.

A number of other parameters were examined to evaluate the differences between the model results with the two boundary layer treatments. Radial variations of several of these parameters are illustrated in Figure 4 for two cases in which the wind speed profiles at the top of the boundary layer were essentially identical ( $T_w = 29\text{C}$  in Table 1).

In the CBL model the stress is determined from the iterative solution for the friction velocity ( $u_{*}$ ), whereas in the bulk transport equation the stress is primarily related to the tangential wind speed at the top of the boundary layer. Nevertheless, the surface shearing stress ( $\tau_0$ ) profiles (Figure 4) were very similar for both models. These values may be compared to  $\tau_0$  estimates by Miller (1962) from data collected in hurricane Helene. Miller calculated the shearing stress necessary to offset the inward momentum transport by the radial wind component, which was estimated from aircraft data at 800 mb and 200 mb. Average  $\tau$  values were 60, 51 and 28 dynes  $\text{cm}^{-2}$  for the radial increments 0-37, 37-74, 74-111 km, respectively. Two factors may explain these large  $\tau$  values compared to those from the model. Miller assumed the surface tangential wind component was equal to the 800 mb value, while a reduction of 0.7 was used in the model. In addition, the radial wind component estimates by Miller were larger than the integrated  $v_r$  values from the model, shown in Figure 4. Thus the transfer to the ocean, or the associated radial divergence of momentum, was smaller for the model results. Experiments in which the drag coefficient (and thus the heat and moisture exchange coefficients) was constant ( $C_D = 2.5 \times 10^{-3}$ ) did not result in different maximum wind speeds. Even though the heat and moisture fluxes at outer radii were increased in these cases, the  $\theta_e$  at the eyewall was largely unaffected. Because the maximum wind speed is determined by the empirical relations (2) - (4), the primary effect of the larger value of  $C_D$  was to increase the frictional stress at the ocean surface, and this was balanced by increased radial advection of momentum. In this respect, the model differs from others (e.g. Rosenthal 1971, Ooyama 1969) in which the ultimate intensity reached by the model storm varies inversely with  $C_D$ .

Another indicator of the storm intensity is the amount of precipitation. In a system such as the hurricane, almost all of the moisture in the inflow

layer is precipitated, since the upper level outflow contains little moisture. An estimate of the precipitation is then the vertical moisture flux through the top of the boundary layer by both the mean and convective motions. The moisture source due to both radial advection and evaporation is included in this precipitation estimate. An integrated radial component of  $3 \text{ m sec}^{-1}$  through the 100 km radius with a moisture content of  $20 \text{ gm kg}^{-1}$  contributes about  $12 \text{ cm day}^{-1}$  to the area-averaged precipitation within that radius. Since evaporation within 100 km of the center adds only another  $1 \text{ cm day}^{-1}$  to the precipitation, the total is closely related to the strength of the inflow. It might be noted that more than 92% of the vertical moisture flux was by the mean vertical motion. Maximum precipitation rates, which occurred at the eyewall, for the bulk transport and the CBL models compared in Figure 4 were  $65$  and  $30 \text{ cm day}^{-1}$ , respectively.

#### Heat Extraction from Ocean

Because the model is eventually to be used to simulate changes in ocean thermal structure changes due to the passage of a tropical cyclone, the total heat extraction and its radial distribution are important considerations. Black and Mallinger (1972) have recently summarized various estimates of the heat flux from the ocean. These estimates were based on bulk transport equations with surface temperatures, moistures and winds extrapolated from aircraft measurements. Maximum fluxes occurred near the radius of maximum winds, with the estimates ranging from less than 800 to more than 6000  $\text{cal cm}^{-2} \text{ day}^{-1}$ . As Black and Mallinger point out, in many of these flux calculations the sea surface temperatures were assumed equal to pre-storm values, and thus may overestimate the flux. A second feature of these calculations was the rapid decrease in heat flux with increasing radius. Nearly all of the flux estimates at five times the radius of maximum winds were less than



one-half of the peak values. Similar variations of total heat flux are evident in the model results shown in Figure 4. Maximum values occur within a few km of the radius of maximum winds, but are considerably smaller than estimates based on empirical data. The values in Figure 4 represent the total heat removed in the first 24 hours of the calculation, with the storm stationary and the ocean temperature fixed. Maximum values of instantaneous latent and sensible heat fluxes at 24 hours were  $1.63 \times 10^{-2}$  and  $0.31 \times 10^{-2} \text{ cal cm}^{-2} \text{ sec}^{-1}$ . Thus the Bowen ratio near the eyewall was about 20%. By contrast, near 300 km the Bowen ratio was approximately 5%. It should be noted that the heat and moisture exchange coefficients were equal to  $2/3 C_D$  in the model with the bulk transport equations, since it was expected that the molecular exchange of heat and moisture at the interface would be inhibited compared to the momentum exchange (Robinson, 1966). A series of experiments was also run with the heat and moisture coefficients equal to the  $C_D$  value. Latent and sensible heat fluxes were, of course, increased by at least 50%. Extreme values of heat removal ranged from 650 to 6200  $\text{cal cm}^{-2} \text{ day}^{-1}$  for ocean temperatures of 27 and 31C, respectively. However, the differences in the temperature fields were less than 0.5C, with warming at large radii and enhanced cooling near the center. The maximum wind speeds were increased by only 3-4  $\text{m sec}^{-1}$  over the values shown in Table 1. Associated increases in  $T_0$ ,  $v_r$  and maximum precipitation rate were also noted. It thus appears that the intensity of the storm produced by the bulk transport model is rather insensitive to exchange coefficients. Specifying coefficients greater than the minimum values necessary to establish the  $\delta\theta_e$  possible for a particular ocean temperature produces proportionately larger heat extraction, but not significantly more intense storms. In future experiments with the ocean surface

temperatures predicted by the heat balance, the variation of  $C_H$  might be expected to have a larger effect. Perhaps one method for determining these exchange coefficients will be to determine the oceanic heat loss from expendable bathythermograph traces as Black and Mallinger (1972) have done for Hurricane Ginger. Calculation of the oceanic heat budget may be more reliable than the use of bulk transport equations with assumed exchange coefficients and with surface winds, temperatures and moistures extrapolated from aircraft data.

The total heat flux after 24 hours in the CBL model was generally smaller than that calculated in the bulk transport version (see Figure 4). Although accurate observations of the heat flux within the hurricane boundary layer are not available, the heat fluxes from the two models appear to be underestimates, especially at outer radii. A lower heat flux may have been a result of the assumption that the total heat flux was proportional to the density (or virtual temperature) gradient near the air-water interface. In the mid-latitudes the stability is primarily determined by the large air-sea (or air-land) temperature differences, and the moisture content is generally not thought to be important. However, in the tropics significant latent heat exchange can occur with rather small air-sea temperature differences. Assuming similarity between the wind and virtual temperature profiles allows heat transfer even if the air and sea temperatures are equal, but it may contribute to an underestimate of the total heat flux. Another factor in the heat flux relation [see (16)] is the ratio ( $a_h$ ) of the eddy conductivity ( $K_H$ ) to the eddy viscosity ( $K_M$ ), which is constant if the profiles are similar. However, the value of the ratio over the sea is not well known. Thus it has been considered a disposable parameter in the model. In a sense this is analogous

to the experiments described above in which the heat and moisture coefficients were varied relative to  $C_D$ . Another explanation for the low heat flux estimates could be that the  $u_*$  or stress values are underestimated. The key relation for the surface roughness parameter as a function of  $u_*$  may also be varied to increase the frictional drag at the surface. This was the second approach used to test the two-layer model. Point values of several parameters are provided in Table 2 from the runs with  $T_w = 29C$ . The surface roughness coefficient ( $C_2 = 0.00428$ ) in (13) and the ratio of heat conductivity to eddy viscosity were also varied in runs for the other sea surface temperatures, and the resulting changes were similar.

Enhancement of the heat exchange relative to momentum exchange (Exp.B) increased the maximum wind speed about 4 m/sec. This increase in maximum wind speed ranged from 3 to 7 m/sec for a  $T_w$  range of 27 to 31C. As in the case of the bulk aerodynamic model, the increase in surface heat exchange beyond a certain critical value does not dramatically change the predicted intensity of the storm for a given  $T_w$ . The need for observational data to determine the proper  $K_M/K_H$  ratio is again evident. Increasing the surface roughness in the model (Exp.C) also resulted in more intense storms, with the increase in intensity ranging from 2 to 4 m/sec for  $T_w$  values between 27 and 31C. As indicated earlier, increases in the surface stress in this model tends to increase the supply of energy through radial advection without greatly retarding the wind speeds at the top of the boundary layer.

A general increase in the values of the parameters in Table 2 may be expected with the increase in  $v_\theta$ , for example, the larger radial component. However, in Exp. C,  $v_r$  was increased by about 35% over the control value, compared to a 10% increase in Exp. B. The stress was about 40% larger with an implied drag coefficient of  $6.4 \times 10^{-3}$  near the center in Exp. C. Even



at 300 km the drag coefficient was  $2.0 \times 10^{-3}$ . The associated inflow angles (ranging from 14 to 27 degrees) and ratio of the velocity at the top of the surface layer to that at the top of the boundary layer near the center were also significantly changed from the control run values. By contrast, the above factors related to the predicted wind fields in Exp. B were not changed beyond the expected variations due to the increased maximum wind speed.

The total heat removed from the ocean in Exps. B and C was larger than in the control run. As expected, the increase was about 50% when the  $K_H/K_M$  ratio was increased from 2 to 3. Peak values ranged from 410 and  $3940 \text{ cal cm}^{-2} \text{ day}^{-1}$  for  $T_w$  equal to 27 and  $31^\circ\text{C}$ , respectively. Enhancement of the momentum exchange at the surface produced correspondingly larger heat fluxes, with the peak values ranging from 420 to greater than  $4670 \text{ cal cm}^{-2} \text{ day}^{-1}$  for the same  $T_w$  values. The larger precipitation rate near the center in Exp. C is evidently due more to a larger  $v_r$  value than to the increase in heat gain, because the 50% larger heat gain in Exp. B is accompanied by only a 20% increase in precipitation rate. This is consistent with the primary moisture source being at larger radii. The inflow angles and implied drag coefficients in Exp. C appear excessive, particularly at outer radii where more observations are available for comparison. The mechanism through which the heat transfer is enhanced is probably in the wind-generated spray (Riehl, 1954), which exposes a much greater surface area for heat transfer from the water to the air. It appears that the momentum exchange is not correspondingly enhanced by the blowing spray (see Monahan 1966, and Wu 1973). If this is the case, the ratio of  $K_H/K_M$  may be a function of the amount of spray, or the surface roughness. This could be incorporated in the model, and would likely

increase the maximum wind speed a small amount. A different representation of the heat loss from the ocean versus radius would also result. The flexibility of the CBL model, and the fact that future research results from air-sea interaction studies will likely be cast in the framework of similarity theory, or external parameters such as  $Z_0$ , is thought to be sufficient to justify this more complex and time-consuming boundary layer model.

## CONCLUDING REMARKS

### Summary

An empirical wind profile and an expression for the maximum wind speed in terms of the radial increase in  $\theta_e$  have been used to specify the winds at the top of the boundary layer in a symmetrical hurricane. Using these winds with the bulk aerodynamic transport equations, and as an input to a two-layer, baroclinic marine boundary layer model by Cardone (1969), solutions have been obtained for the moisture and potential temperature distributions within the boundary layer. The vortex in turn responds to the equivalent potential temperature gradient induced by the balance between the heat/moisture sources and the advection by the boundary layer winds. Equilibrium maximum wind speeds vary from minimal hurricane force to  $80 \text{ m sec}^{-1}$  for ocean temperatures between 27C and 31C. This might be considered the maximum storm for the specified ocean conditions; in actual storms the external environmental effects would determine if these wind speeds would be achieved. For a given ocean temperature, maximum wind speed in the model is shown to be very sensitive to the maximum relative humidity of the surface air near the eyewall, which is specified as an external parameter in an attempt to parameterize the convective flux through the top of the boundary layer. The bulk aerodynamic and the Cardone

boundary layer approach give similar maximum wind speeds for the same external conditions. There is a certain arbitrariness in the total heat flux from the ocean for a given viscosity in both boundary layer versions. Observations of heat loss from the ocean are needed to establish the appropriate constants in the high wind speed conditions that characterize hurricanes. Various parameters predicted by the Cardone model, such as the radial mass flow and inflow angles, depth of the boundary layer, vertical motion and turbulent fluxes, may be evaluated by aircraft equipped with inertial guidance systems that are available.

#### Possible Applications of the Model

The original objective was to develop an atmospheric vortex capable of simulating the effect of a hurricane on the ocean thermal structure. Since the ocean temperature affects the intensity of the vortex, a mutual interaction may occur if significant cooling occurs in the ocean. Leipper and Volgenau (1970) suggested that the subsurface thermal structure must also be considered in forecasting intensity changes in hurricanes. Many experiments are planned to evaluate the effect of gradients in both sea surface temperature and thermocline depth. A layer ocean model similar to that used by Kraus and Turner (1967) is to be tested.

The adjustment time in the model is relatively short (see Figure 5). For  $T_w = 31^\circ\text{C}$ , the increase in  $v_{\theta\text{max}}$  from 30 to 70  $\text{m sec}^{-1}$  occurred within 11 hrs. Thus the model experiments can be run with a variety of sea temperature conditions. In the present form the vortex is stationary, so that allowing the sea temperature to vary will simulate the rate of decay of the vortex due to cooling at inner radii. The method of moving the vortex will be based on the integrating effect of strong tangential winds in producing properties which are nearly axisymmetric. Application of the

two-dimensional model along four or more diagonals will be used to estimate the symmetric component--which determines the intensity of the storm. In this way the model vortex may be moved over a varying ocean thermal field. One advantage of the present model over previous numerical models is the possibility of simulating the symmetric component of actual storms. The model can be initialized to a particular maximum wind speed by adjusting the exchange coefficients or other external parameters, for the specified ocean temperature. Experiments are planned to test this capability with real data by moving the model storm along the actual track with the external parameters held constant. One should then be able to assess the predicted changes in maximum intensity of the storm and in the ocean thermal structure.

Finally, the model could be useful in testing proposed hurricane modification schemes that are dependent on reduction of the interface fluxes of heat and moisture, or the inflow within the boundary layer. It has been proposed (Project Stormfury 1968) that spreading of mononuclear films could inhibit evaporation from the ocean and thus reduce the energy source for hurricanes. Results from the model verify this reasoning, particularly if the moisture content reduction could be maintained in the inner region of the storm. With currently available organic materials, the film is dispersed by the high wind speeds. It might be possible to efficiently test many patterns of material spreading to determine the most effective. There may be some optimum radius beyond which the materials cannot be economically laid down for a given benefit from reducing the maximum wind speed. A more recent proposal by Gray (1973) to modify the hurricane by carbon dust seeding within the boundary layer might also be tested with this model. Gray's hypothesis is that artificial warming of the atmosphere

boundary layer due to absorption of insolation by the carbon dust may cause an additional mass flux out of the boundary layer. A decrease in the low-level inflow is expected to decrease the inner core maximum wind velocities, and thus reduce the storm damage. The potential benefit of the various hurricane modification schemes is enormous--and so also is the possible damage from misguided attempts. Wherever possible, these schemes should be tested on a variety of numerical models, including the type proposed here.

#### Acknowledgements

This research has been partially supported by the Environmental Prediction Research Facility, Monterey, California and by the Office of Naval Research (NR 083-275-5). Numerous discussions with Drs. K. Davidson and R. Haney of the Department of Meteorology, Naval Postgraduate School, and Dr. J. Kaitala and LT. D. McConathy of Fleet Numerical Weather Central, Monterey, were very beneficial in applying the boundary layer model which Dr. V. Cardone, New York University supplied. Prof. D. Leipper and Dr. E. J. Harrison, Jr. also offered helpful comments on the manuscript, which was typed by Miss M. Marks. The basis for this research was developed during the early years of the author's career under the tutelage of Prof. Herbert Riehl, Colorado State University.



## REFERENCES

- Anthes, R. A., S. L. Rosenthal and J. W. Trout, Preliminary results from an asymmetric model of the tropical cyclone, Mon. Wea. Rev., 99, 744-758, 1971.
- Black, P. G., and W. D. Mallinger, The mutual interaction of hurricane Ginger and the upper mixed layer of the ocean, 1971 Project Stormfury Annual Report, NOAA, 1972.
- Blackadar, A. K., A simplified two-layer model of the baroclinic neutral atmosphere boundary layer, Air Force Cambridge Research Laboratories Report 65-531, 49-65, 1965.
- Bell, G. J., and Tsui, Kao-Sing, Some typhoon soundings and their comparison with soundings in hurricanes, J. Appl. Meteorol., 9, 74-93, 1973.
- Cardone, V., Specification of the wind distribution in the marine boundary layer for wave forecasting, Geophysical Sciences Laboratory TP 69-1, New York Univ., 131 pp., 1969.
- Gray, W. M., Feasibility of beneficial hurricane modification by carbon dust seeding, Atmospheric Science Paper No. 196, Colorado State University, 130 pp., 1973.
- Gray, W. M., and D. J. Shea, The hurricane's inner core region; II. Thermal stability and dynamic characteristics, J. Atmos. Sci., 30, 1565-1576, 1973.
- Kraus, E. B., and J. S. Turner, A one-dimensional model of the seasonal thermocline, II, Tellus, 19, 98-105, 1967.
- Leipper, D. F., and D. Volgenau, Hurricane heat potential of the Gulf of Mexico (Abstract), Transactions, Am. Geophys. Union, 51, 312, 1970.
- Marcus, S. O., Jr. and A. L. Smith, Jr., Evaluation of data received from Navy NOMAD's in 1964, National Geographic Data Center Report, Washington, D. C., 46 pp., 1966.
- Miller, B. I., On the momentum and energy balance of hurricane Helene (1958), National Hurricane Research Project Report No. 53, 19 pp., 1962.
- Monahan, E. C., Sea spray and its relationship to low elevation wind speed, Ph.D. Thesis, Mass. Inst. Tech., Cambridge, 1966.
- Ooyama, K., Numerical simulation of the life-cycle of tropical cyclones, J. Atmos. Sci., 26, 3-40, 1969.
- Project Stormfury, Annual report, Department of the Navy and Department of Commerce, 17 pp., 1968.

- Riehl, H., Some relations between wind and thermal structure of steady-state hurricanes, J. Atmos. Sci., 20, 276-287, 1963.
- Robinson, G. D., Another look at some problems of the air-sea interface, Quart. J. Roy. Meteorol. Soc., 92, 451-465, 1966.
- Rosenthal, S. L., The response of a tropical cyclone model to variations in boundary layer parameters, initial conditions, lateral boundary conditions, and domain size, Mon. Wea. Rev., 99, 767-777, 1971.
- Shea, D. J., and W. M. Gray, The hurricane's inner core region; I. Symmetric and asymmetric structure, J. Atmos. Sci., 30, 1544-1564, 1973.
- Wu, J., Spray in the atmospheric surface layer: Laboratory study, J. Geophys. Res., 78, 511-519, 1973.
- Yamasaki, M., A tropical cyclone model with parameterized vertical partition of released latent heat, J. Meteorol. Soc. of Japan, 46, 202-214, 1968a.
- Yamasaki, M., Detailed analysis of a tropical cyclone simulated with a 13-layer model, Papers in Meteorology and Geophysics, 19, 559-585, 1968b.



TABLE 1. Maximum wind speed (m/sec) in the model as a function of sea temperature for the two boundary layer versions. The critical moisture distribution was by specification of the cloud base or by the maximum relative humidity. Values in parentheses indicate speed if environmental  $\theta_e$  values exceeding 350K are used in Eq. (5) rather than a fixed  $\theta_e = 350K$  at  $r_o$ .

Ocean Temperature (deg C)	Bulk Aerodynamic Moisture Specification		CBL Moisture Specification	
	Cloud base	75 to 95%	Cloud Base	75 to 95%
31	70	76	65(51)	76(62)
30	58	64	56(47)	66(61)
29	48	56	44(43)	56
28	36	47	32	46
27		36		33

TABLE 2. Significant parameters at inner (I), middle (M) and outer (O) regions from CBL model upon variation of the surface roughness (coefficient C2) and the ratio of heat conductivity to eddy viscosity ( $a_h$ ). Ocean temperature held fixed at 29C.

Variable	Region	Experiment		
		A	B	C
C2	-	0.00428	0.00428	0.025
$a_h$	-	2	3	2
$v_\theta$ [m sec <sup>-1</sup> ]	I	56.5	60.5	58
$v_r$ [m sec <sup>-1</sup> ]	I	1.4	1.5	1.9
Stress [dyne cm <sup>-2</sup> ]	I	37	43	50
$\frac{V_h}{v_\infty}$	I	.60	.62	.50
	O	.85	.83	.82
Inflow	I	22	23	27
Angle [deg]	O	10	10	14
$C_D \times 10^3$	I	2.9	3.1	6.4
	O	1.1	1.0	2.0
Precip [cm day <sup>-1</sup> ]	I	33	38	51
Total heat removed	I	980	1460	1670
[cal cm <sup>-2</sup> day <sup>-1</sup> ]	M	180	100	115

## LIST OF ILLUSTRATIONS

- Figure 1. Schematic model of atmospheric vortex and associated inflow layer. The exponent  $x$  is  $-1$  within  $r_i$  and  $1/2$  between  $r_i$  and  $r_o$  (see text).
- Figure 2. Schematic of the Cardone (1969) boundary layer model.
- Figure 3. Radial variation of the air minus sea temperatures for the CBL with the ocean temperature fixed at 27, 29 and 31C. The curves indicate the steady state values with the ocean temperature held fixed.
- Figure 4. Comparison of radial profiles of selected parameters from the bulk aerodynamic boundary layer equations (solid line) and the Cardone (CBL) model (dashed). The radial velocity at the top of the surface layer ( $v^*$ ), from the CBL model is shown in the middle panel.
- Figure 5. Variation of maximum wind speed, starting from an initial wind speed of  $30 \text{ m sec}^{-1}$ , for different ocean temperatures. The arrows indicate the time at which the specific humidity value at the eyewall first exceeded the critical relative humidity.

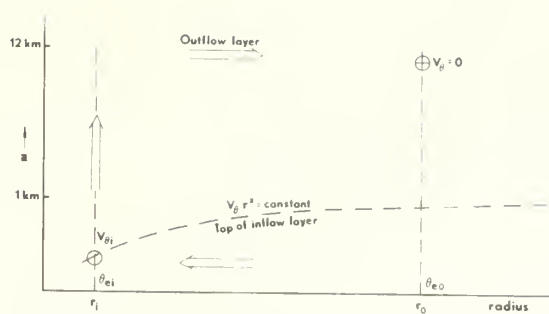


Figure 1. Schematic model of atmospheric vortex and associated inflow layer. The exponent  $x$  is  $-1$  within  $r_i$  and  $1/2$  between  $r_i$  and  $r_0$  (see text).

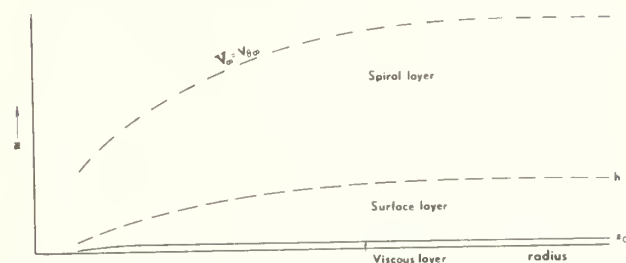


Figure 2. Schematic of the Cardone (1969) boundary layer model.

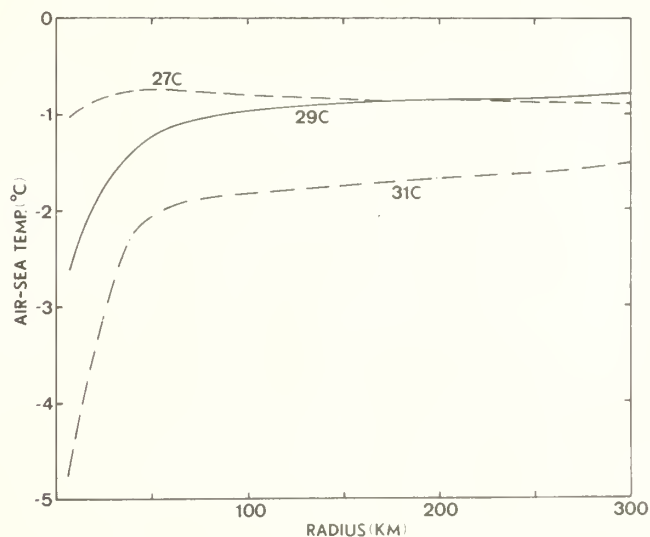


Figure 3. Radial variation of the air minus sea temperatures for the CBL with the ocean temperature fixed at 27, 29 and 31C. The curves indicate the steady state values with the ocean temperature held fixed.

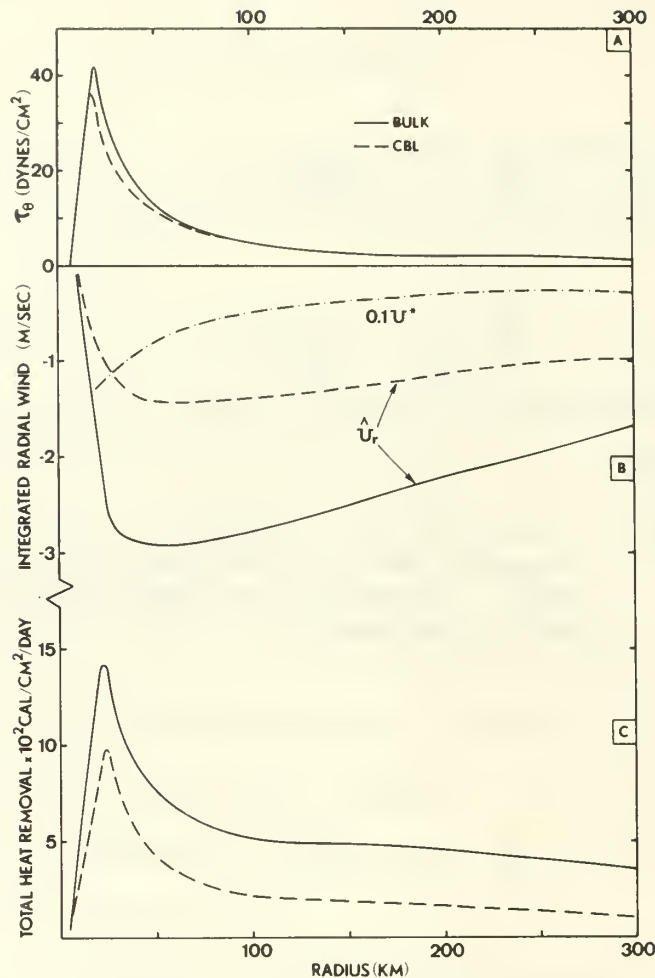


Figure 4. Comparison of radial profiles of selected parameters from the bulk aerodynamic boundary layer equations (solid line) and the Cardone (CBL) model (dashed). The radial velocity at the top of the surface layer ( $v^*$ ), from the CBL model is shown in the middle panel.

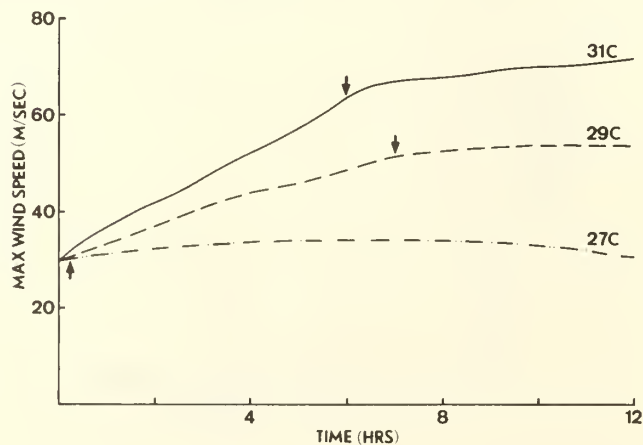


Figure 5. Variation of maximum wind speed, starting from an initial wind speed of  $30 \text{ m sec}^{-1}$ , for different ocean temperatures. The arrows indicate the time at which the specific humidity value at the eyewall first exceeded the critical relative humidity.

# DISTRIBUTION LIST

	No. Copies
1. Director of Defense Research and Engineering Office of the Secretary of Defense Washington, D. C. 20301 ATTN: Office, Assistant Director (Research)	1
2. Office of Naval Research Arlington, Virginia 22217 ATTN: (Code 480) ATTN: (Code 460) ATTN: (Code 102-OS)	3 1 1
3. Director Naval Research Laboratory Washington, D. C. 20390 ATTN: Library, Code 2029 (ONRL) ATTN: Library, Code 2620	6 6
4. Defense Documentation Center Cameron Station Alexandria, Virginia 22314	12
5. Commander Naval Oceanographic Office Washington, D. C. 20390 ATTN: Code 1640 ATTN: Code 70	1 1
6. NODC/NOAA Rockville, Maryland 20882	1
7. Office of Naval Research Branch Office 1030 E. Green Street Pasadena, California 91106	1
8. Environmental Prediction Research Facility Naval Postgraduate School Monterey, California 93940	2
9. Library, Code 0212 Naval Postgraduate School Monterey, California 93940	2
10. Professor R. L. Elsberry, Code 51Es Naval Postgraduate School Monterey, California 93940	6
11. Professor D. F. Leipper, Code 58Lr Naval Postgraduate School Monterey, California 93940	1

- |     |  |   |
|-----|--|---|
| 12. | LCDR N. A. S. Pearson<br>Helicopter Support Squadron Seven<br>Naval Air Station Imperial Beach<br>Imperial Beach, California 92032 | 1 |
| 13. | LCDR B. Corgnati, Jr.<br>77 Malcolm Road<br>North Kingstown, Rhode Island 02852  | 1 |
| 14. | Department of Meteorology<br>Code 51<br>Naval Postgraduate School<br>Monterey, California 93940                                    | 2 |
| 15. | Dean of Research<br>Monterey, California   | 1 |



SECURITY CLASSIFICATION OF THIS PAGE (When Data Entered)

REPORT DOCUMENTATION PAGE		READ INSTRUCTIONS BEFORE COMPLETING FORM
1. REPORT NUMBER NPS-51Es74011A	2. GOVT ACCESSION NO.	3. RECIPIENT'S CATALOG NUMBER
4. TITLE (and Subtitle) A Quasi-empirical Model of the Hurricane Boundary Layer		5. TYPE OF REPORT & PERIOD COVERED Jan-Dec 1973
		6. PERFORMING ORG. REPORT NUMBER
7. AUTHOR(s) Russell L. Elsberry Nils A.S. Pearson Leino B. Corgnati, Jr.		8. CONTRACT OR GRANT NUMBER(s) Proj Order No. P04-0121 Research Project RR 131-03-01
9. PERFORMING ORGANIZATION NAME AND ADDRESS Naval Postgraduate School Monterey, California 93940		10. PROGRAM ELEMENT, PROJECT, TASK AREA & WORK UNIT NUMBERS Program Element 61153N Task NR 083-275-05
11. CONTROLLING OFFICE NAME AND ADDRESS Office of Naval Research Code 400P and Code 481 Arlington, Virginia 22217		12. REPORT DATE 31 January 1974
		13. NUMBER OF PAGES 34
14. MONITORING AGENCY NAME & ADDRESS (If different from Controlling Office)		15. SECURITY CLASS. (of this report) Unclassified
		15a. DECLASSIFICATION/DOWNGRADING SCHEDULE
16. DISTRIBUTION STATEMENT (of this Report)  Approved for public release; distribution unlimited.		
17. DISTRIBUTION STATEMENT (of the abstract entered in Block 20, if different from Report)		
18. SUPPLEMENTARY NOTES This research was sponsored in part by the Environmental Prediction Research Facility, Monterey, California and the Office of Naval Research.		
19. KEY WORDS (Continue on reverse side if necessary and identify by block number) Hurricane model Tropical meteorology Boundary layer model Air-sea interaction		
20. ABSTRACT (Continue on reverse side if necessary and identify by block number) Solutions have been obtained for the temperature and moisture distributions within the atmospheric boundary layer of an axisymmetric hurricane model. The intensity of the hurricane is related to the equivalent potential temperature gradient produced by a balance of heat sources and advection within the boundary layer. Solutions are obtained using the bulk aerodynamic transport equations or applying a two-layer, baroclinic boundary layer model by Cardone (1969). Equilibrium maximum wind speeds vary from minimal hurricane force to about 80 m/sec for fixed ocean temperatures between 27C and .		

31C. Observations of the oceanic heat loss in actual storms are necessary to establish the ratio of heat flux to momentum transfer in the high wind speeds treated by the model. Various applications of the model are proposed, with an ultimate goal of a time-dependent simulation of hurricane-ocean coupling.

U158644

DUDLEY KNOX LIBRARY - RESEARCH REPORTS



5 6853 01060502 5

U1506